JOURNAL OF MATERIALS SCIENCE 30 (1995) 6136–6144

Ultrasonic spray pyrolysis of a chelated precursor into spherical $YBa_2Cu_3O_{7-x}$ high temperature superconductor powders

C. H. CHAO, P. D. OWNBY*
*Departments of Electrical and Computer Engineering, University of Missouri, Columbia, MO 65211, and *Ceramic Engineering, University of Missouri, Rolla, MO 65401, USA*

$YBa_2Cu_3O_{7-x}$ powders have been prepared directly by ultrasonic spray pyrolysis using nitrate salts as precursors and citric acid and ethylene glycol as chelating agents. This method consists of ultrasonically atomizing a precursor solution into droplets, thermally chelating, drying, decomposing and solid state reacting these droplets in a carrier gas flowing through a tube furnace, forming a well characterized powder. The chelated precursor adjusted to pH 8 forms bidentate bonding between the cations and the chelating agents. Thermal analysis and infrared spectroscopy identify the decomposition steps of the precursor. The dry gel of the chelated precursor is nearly amorphous indicating intimate mixing on the atomic level. X-ray diffraction suggests the mechanism of forming the 1:2:3 crystalline phase. Spherical powders are produced with diameters ranging from 0.2 to 0.8 μm depending on the ultrasonic frequency and the solution concentration. The spherical particles are hollow or solid depending on the precursor type and the furnace temperature. The primary crystallite size is about 10–50 nm. X-ray diffraction data and infrared spectra show that the spray pyrolysed powder from the chelating precursor forms the $YBa_2Cu_3O_{7-x}$ phase at 800 °C, which is 100 °C lower than that formed from unchelated precursors.

1. Introduction

Current fabrication techniques for producing reliable electronic and structural ceramic components require the use of a near ideal starting powder, which is considered to be a fine particle size, non-agglomerated, spherical, narrow size distributed, high purity powder [1, 2]. A variety of non-conventional synthesis techniques through solution or the vapour phase, such as chemical coprecipitation [3–6], chelating and thermal decomposition [7–10], sol–gel techniques [11–14], hydrothermal precipitation [15], spray pyrolysis [16–19], aerosol reaction [20–22], etc., have been applied in attempts to synthesize powders that meet these idealized criteria [23]. However, most products of these techniques are metal salts or hydroxides, generally in the form of hard and soft agglomerates, which need further calcination to obtain the fully reacted oxide powders.

Both chelated and sol–gel precursors can be used in solutions for this process. With sol–gel precursors, homogeneous yttria-stabilized zirconia powders [21] and fine, spherical ZrO_2–SiO_2 particles [22] have been prepared by ultrasonic spray pyrolysis of alkoxide solutions. For spray pyrolysis of aqueous solutions, only the effect of additives [16] and the effect of anions on the particle morphology [17–19] have been investigated. Even more recently, multicomponent oxide powders synthesized by spray pyrolysis in both the laboratory and on an industrial scale have employed only the salt solutions of the components [24–28], which lead to the aggregation of each salt in the sprayed droplets due to

1. separate precipitation of each salt of different solubility,
2. separate decomposition of each salt at different temperatures, and
3. incomplete solid state diffusion reactions among the components in the very short pyrolysis period in the tube furnace and at the very slow reaction rates between each aggregation of salt.

In the spray pyrolysis process of a chelated multicomponent precursor, chelation or polymerization of the cations should result in atomic level intermixing between cations. The chelating or polymerizing agents should be able to hold the cations together, resulting in an amorphous, clear gel. The decomposition of a gel is exothermic due to the combustion of the metal–organic chelated compound. Heat evolution should help the solid state reaction among cations to proceed. Solutions prepared for spray pyrolysis of a multicomponent system with a properly selected chelating agent will, therefore, in principle, lead to a homogeneously dried, decomposed and fully reacted, spherical, single phase, ceramic oxide powder. Particle size can be controlled

*Author to whom correspondence should be addressed.

0022–2461

by the solution concentration and the ultrasonic atomization frequency. The resulting particles may be hollow or solid spheres depending on the pyrolysis temperature, solution concentration, type of precursor and initial solution droplet size [29].

Consequently, there should be no necessity for further calcination. Therefore, it should be possible to synthesize high purity, single phase, fine particle size, spherical, uniformly distributed, reactive ceramic powders for final sintering of technical ceramic components by controlling the parameters of the process (chelating agent, solution concentration, atomization, carrier gas flow rate, pyrolysis temperature, atmosphere, etc.). In this paper, $YBa_2Cu_3O_{7-x}$ powders have been prepared directly by this ultrasonic spray pyrolysis method demonstrating this thesis.

2. Experimental procedure

2.1. Preparation of solution

The solution precursor for the $YBa_2Cu_3O_{7-x}$ superconductor was prepared by first dissolving 99.99% pure Y_2O_3, $BaCO_3$ and CuO powders, in the atomic Y:Ba:Cu ratio equal to 1:2:3, in an aqueous solution of 0.08 M nitric acid. Six gram equivalents of citric acid and ethylene glycol were then added per equivalence of the precursor solution for stock. Solutions of different pH values adjusted by NH_4OH were heated on a hot plate to simulate spray pyrolysis in a tube furnace until the viscous solutions "puffed-up" indicating carbonate decomposition. The viscous solutions were cooled and dried at 80 °C to gels. The pH range of about 8–9 with the clear blue–green dry gel from solutions was chosen for the spray pyrolysis. These same dried gels from solutions of different pH values were examined by X-ray diffraction for microcrystalline precipitation. Solutions of 0.01 M concentration with the correct pH value with and without chelating agents were prepared for spray pyrolysis.

2.2. Ultrasonic atomization

A commercial ultrasonic humidifier was modified and connected through a copper tube to a tube furnace for the experiments. The frequency of the piezoelectric transducer was adjustable from 1.25 to 1.8 MHz. The prepared solutions were ultrasonically atomized into fine droplets at a rate of about 75 ml per h^{-1}. An air carrier gas at a flow rate of about 20 $cm^3 s^{-1}$ introduced the atomized mist continuously into the tube furnace. Assuming laminar flow, the residence time of the mist was about 20 s.

The size of the droplets in the atomized mist was calculated with the model from Peskin and Raco [30] and for a large solution depth above the transducer, the relation can be simplified as

$$d_o = \left(\frac{4\pi^3\sigma}{\rho\omega_o^2}\right)^{1/3} \quad (1)$$

where d_o is the expected diameter of the droplet (μm); σ, the surface tension of the solution (N cm^{-1}); ρ, the liquid density (g cm^{-3}); and ω_o, the frequency of the transducer (Hz).

Equation 1 shows the correlation between the transducer frequency, the liquid properties and the size of the ultrasonically atomized mist. If it is assumed that one individual droplet will form one oxide particle after spray pyrolysis, then from the conservation of mass relation, the expected particle size of the oxide can be calculated

$$d_{ox} = \left(\frac{M_{ox} \times C \times 10^{-3}}{\rho_{ox}}\right)^{1/3} \times d_o \quad (2)$$

where d_{ox} is the diameter expected after spray pyrolysis (μm); C, the cation concentration of the solution base (mol l^{-1}); ρ_{ox}, the density of the spray pyrolysed powder in (g cm^{-3}); and M_{ox}, the molecular weight of the oxide powder (g mol^{-1}).

2.3. Furnace condition and powder collection

The temperature profile in the tube furnace was measured with a chromel–alumel thermocouple. The alumina muffle tube was 50.8 cm and 3.8 cm internal diameter (i.d.,) with an average constant temperature zone of about 36 cm. The pyrolysed particles were collected by a copper condensation tube and also by bubbling the carrier air through agitated methanol to increase the collection efficiency. A commercial air purifier was also used for the powder collection. The system gas was disposed of through an exhaust system.

2.4. Characterization techniques

Thermogravimetric analysis (TGA) and differential thermal analysis (DTA) were used to study the thermal processes upon heating the dried gels of different pH values, nitrates and organic resins.

Fourier transformed infrared (FTIR) absorption spectra were produced from the dried gels of different pH values and from dried gels decomposed at different temperatures to understand the chelation of the cations and the evolution of the chemistry and mechanisms. The spectra were taken using a Perkin Elmer 1750 infrared fourier transform spectrometer. Infrared absorption peaks were identified with the standard spectra for a more complete understanding of the reactions.

X-ray diffraction (XRD) patterns of the spray pyrolysed powders and the hot plate decomposed samples at different temperatures were obtained with CuK_α radiation and identified.

The particle size, morphology and chemical purity of the particles after ultrasonic spray pyrolysis were examined under a Jeol JSM-35CF scanning electron microscope with energy dispersive spectrometer (SEM–EDSX).

3. Results and discussion

3.1. Reaction mechanism

3.1.1. Thermal analysis

The TGA of the nitrates shows, in Fig. 1, that the copper nitrate precursor decomposes at 200–300 °C, the yttrium nitrate at 300–400 °C and the barium

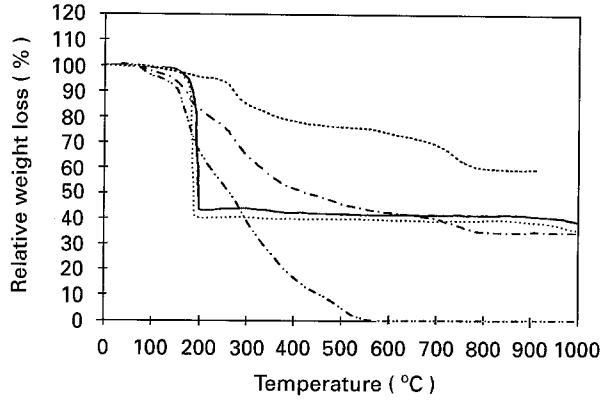

Figure 1 Thermogravimetric analysis of chelated precursors of different pH values compared from (-----) nitrates and (-·-·-) organics: (---) pH < 6, (—) pH 8–9, (.....) pH > 12.

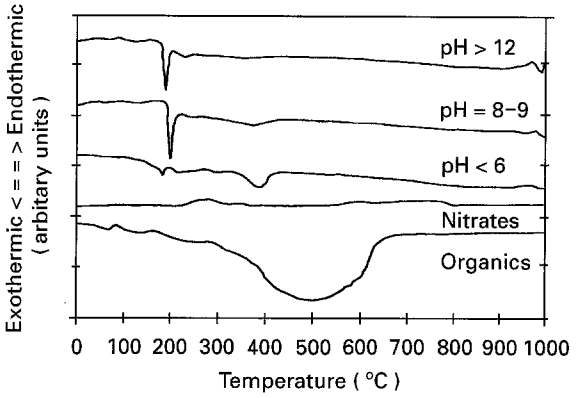

Figure 2 Differential thermal analysis of chelated precursors with different pH values compared from nitrates and organics.

nitrate at 600–800 °C. By adding chelating agents, which are exothermic during decomposition, the decompositions occur at lower temperatures. As the pH value was adjusted by adding ammonia, some chelating effect occurred and the dry gel was decomposed at almost the same temperature, about 200 °C. DTA (Fig. 2) shows that the decomposition of the nitrates had three minor endothermic peaks, while the resin had one main exothermic peak around 400–600 °C. For the chelated precursors, only one main exothermic peak appears at about 180–200 °C.

3.1.2. Chemical bonding identification

The FTIR spectra of the resin chelated precursor with pH < 6, with pH 8 and with pH > 12 are shown in Fig. 3. In the resin, the FTIR spectrum shows the typical ester (R–CO–O–R) characteristics, where the absorption peaks are: C=O stretching at 1736 cm^{-1}, C–O–C asymmetrical bending at 1191 cm^{-1}, C–O–C symmetrical bending at 1079 and 1049 cm^{-1}. The peak representing O–H in-plane bending, one characteristic of an organic acid, is at 1385 cm^{-1}. Water of crystallization shows a peak at 3600–3100 cm^{-1} for O–H stretching and a shoulder at 1633 cm^{-1} for H–O–H bending. Absorption peaks at 3200–2500 cm^{-1} were due to chelation (intramolecular H bond with C=O) overlapped by a C–H stretching vibration.

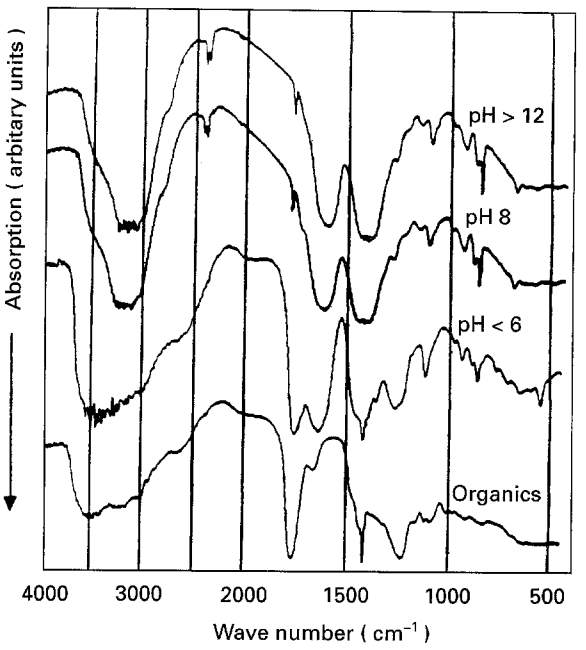

Figure 3 Infrared absorption spectra of chelated precursors of different pH values compared from nitrates and organics.

In the spectrum of the precursor with pH < 6, unidentate complex COO– shows its asymmetrical stretching peak at 1606 cm^{-1}, overlapping a bending peak of H–O–H. The nitrate anion shows its O–NO_2 stretch at 1350–1250 cm^{-1} and the O–N stretching is seen at 850–820 cm^{-1}. Peaks at 726, 667, 606 and 504 cm^{-1} are due to M–O bonding.

In the spectra of precursors with pH 8 and pH > 12, instead of ester and water of crystallization characteristic peaks, antisymmetrical and symmetrical bidentate stretching of C–O show their peaks at 1608–1587 and 1401 cm^{-1}, respectively. Stretching and bending of NH_4^+, show their peaks at 3260–3000 and 1435–1371 cm^{-1}, respectively. Sharp peaks at 2426, 2396 and 1764 cm^{-1} are due to the presence of barium carbonate. These peaks in the spectrum of the precursor with pH < 6 are overlapped by other peaks. Peaks due to the M–O bonding are at 651, 547 and 450 cm^{-1}, which suggests that a different chelation effect occurs than in those with pH < 6.

The FTIR analyses of the chelated precursors at pH 8–9 with temperatures from 25 to 1000 °C are shown in Fig. 4. After decomposition at about 200 °C, the spectrum shows that the nitrate anion is almost completely decomposed and yields peaks of barium carbonate. The 300–700 °C spectra show peaks of barium carbonate. The spectra of the 800–950 °C precursors show the infrared transparency, which is characteristic of the Y–Ba–Cu–O superconducting phase [31]. The 800 °C spectrum shows that the superconducting phase was forming at that temperature.

3.1.3. Bulk phase evolution

X-ray diffraction patterns of precursors dried at 80 °C show evidence of the formation of ammonium nitrate and the "dissolution" of most of the barium nitrate into an amorphous form (Fig. 5). The XRD patterns

characterized phase evolution of chelated precursors from 200 to 800 °C, shown in Fig. 6, and can be compared to those of nitrate precursors in Fig. 7. These figures show the different decomposition routes of the precursors. From chelated precursors, the superconducting phase started to form at 750 °C and was well reacted to a single phase at 800 °C; while from the nitrate precursors, the same phase formed more gradually up to 800 °C and above. The results confirm atomic-level intermixing between cations in the chelated precursor.

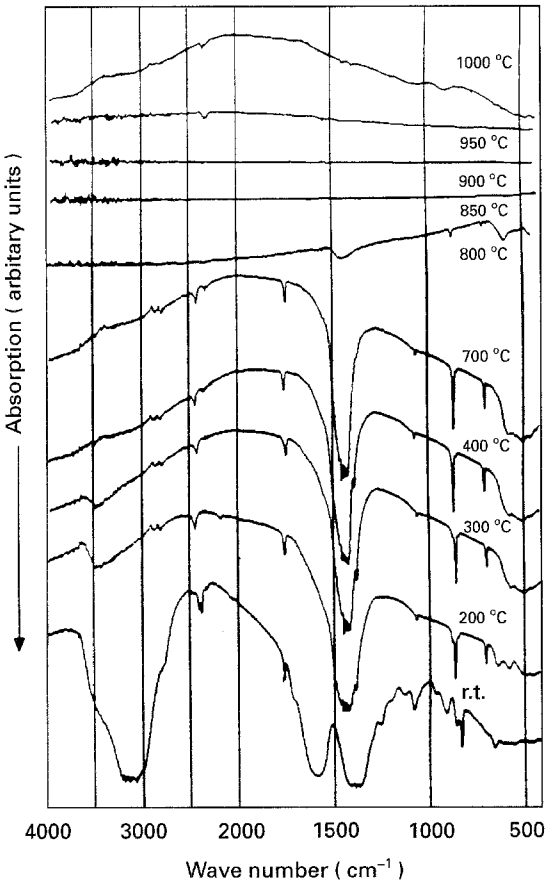

Figure 4 Infrared absorption spectra of chelated precursors with pH 8 decomposed at different temperatures.

3.2. Powder characterization

3.2.1. Particle size and morphology

The morphologies of powders from precursors at various temperatures are normally spherical and either hollow or solid depending on the pyrolysis temperatures. Mean particle size from the chelated precursors decreased at pyrolysis temperatures from 800 to 850 °C, indicating complete formation of the superconducting phase as temperature increased. At 900 °C, the mean particle size and its standard deviation increased due to the onset of melting the superconducting phase and the consequent agglomeration of the particles. The particle size decreased above 950 °C suggesting partial melting of the hollow particles into solid particles. For the particles from nitrate precursors, the mean size remained unchanged due to non-reacted oxides at 800 and 850 °C, and then decreased at 900 °C due to decomposition of barium carbonate and to forming the 1 : 2 : 3 superconducting phase. The increased particle size at 950 °C is due to melting and agglomeration, and finally the decrease at 1000 °C is due to the melting of hollow particles into solid particles. The change of the median size of the spray pyrolysed particles of both precursors at different temperatures is shown in Fig. 8.

A uniform particle size distribution of the superconducting powders is shown in Fig. 9. Primary, secondary

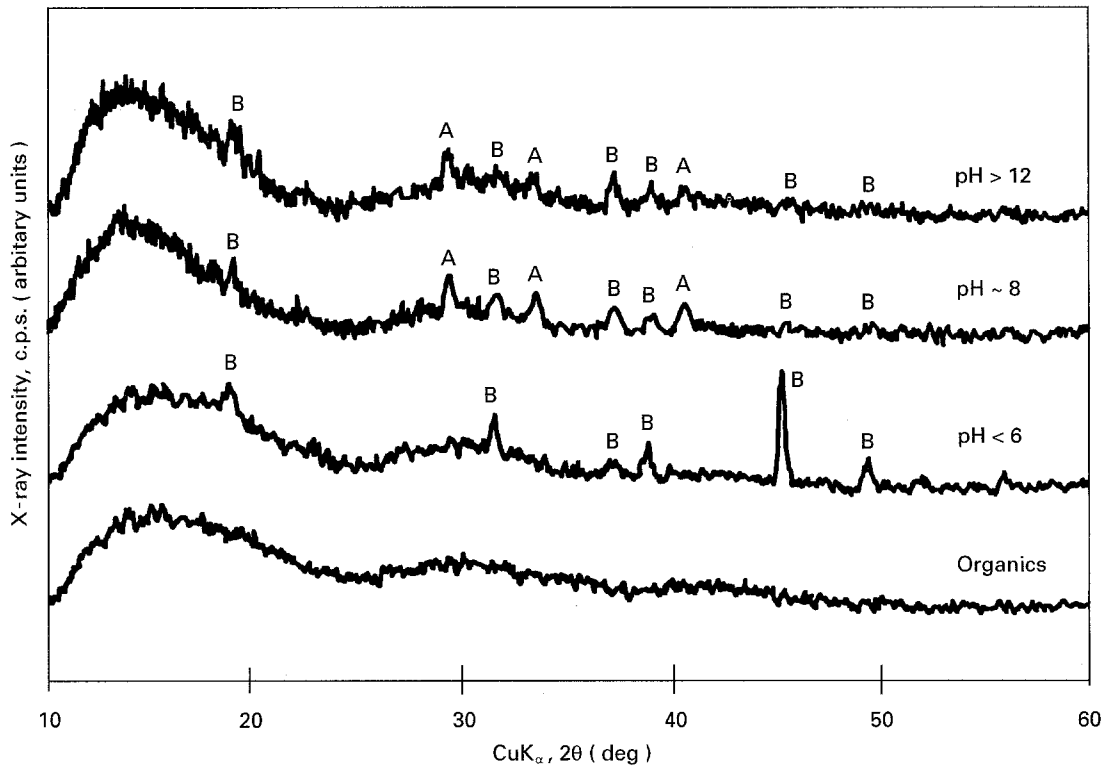

Figure 5 X-ray diffraction patterns of dried chelated precursors of different pHs: (A) ammonia nitrate, (B) barium nitrate.

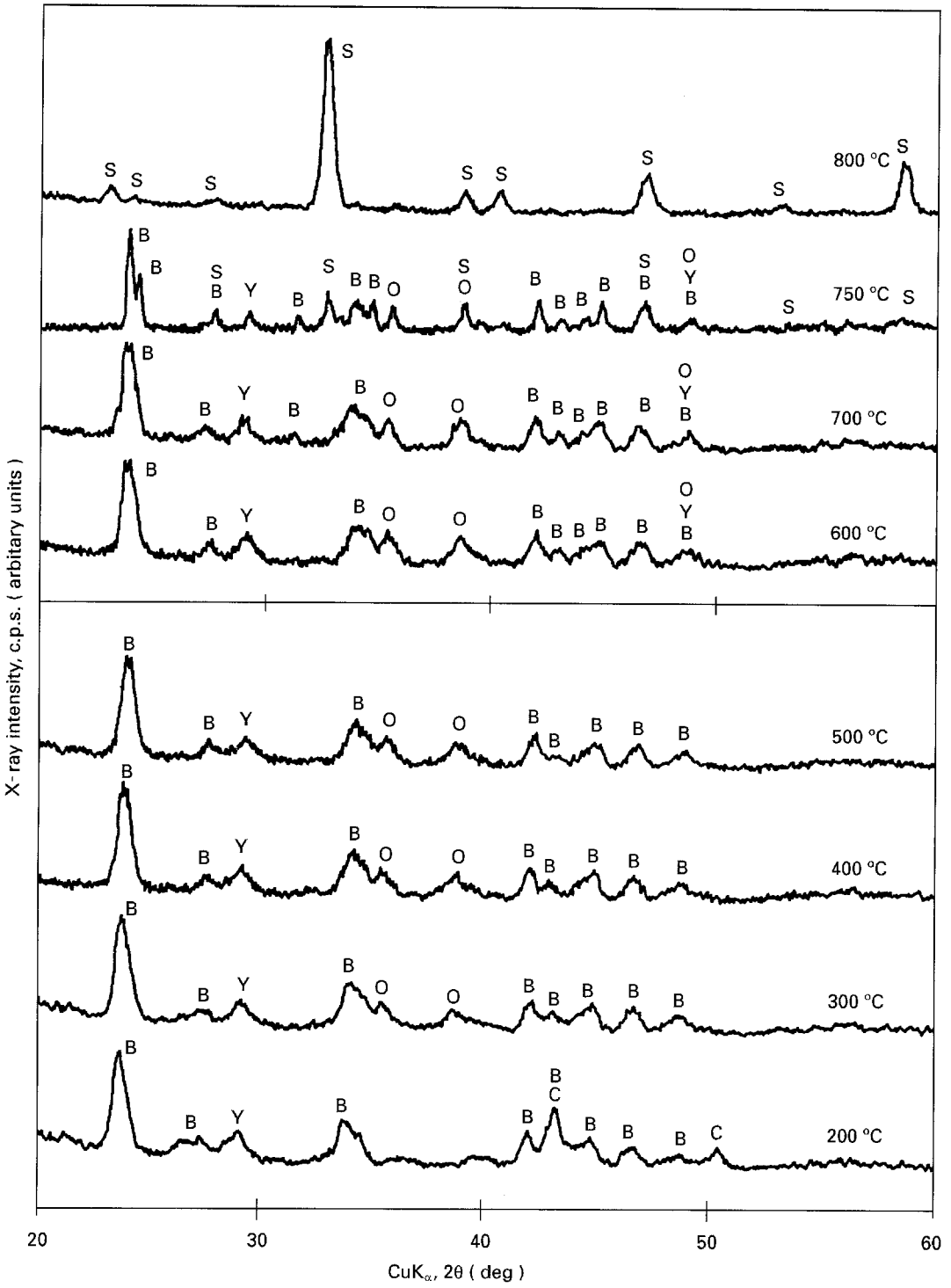

Figure 6 X-ray diffraction patterns of thermally decomposed chelated precursors with pH 8 at 200–800 °C: (Y) Y_2O_3, (S) $YBa_2Cu_3O_7$, (O) CuO, (B) $BaCO_3$, (C) Cu.

and agglomerated particles are shown in Fig. 10. The secondary particles have an orange-peel surface with the grain size similar to the size of the primary particles (Fig. 11). The agglomerated particles consist of secondary particles, and their morphology may or may not be spherical. Calculation of the particle size via Equation 2 using an ultrasonic frequency of 1.4 MHz, a liquid density of 1.05 g cm^{-3} and a liquid surface tension of 12.7 Mn cm^{-1}, yields a liquid droplet size before pyrolysis of about 2 μm. From Equation 2, assuming full density of the superconducting phase in the particle, the corresponding particle size should be about 0.1 μm. Considering the effect of the hollow spheres, a reasonable range of particle sizes is from 0.2 to 0.5 μm, which is the size of secondary particles measured from micrographs.

The calculations from the equations and the morphology from the SEM micrographs enable one to estimate the particle formation mechanism from ultrasonic spray pyrolysis of the precursors. Fig. 12 shows the broken hollow sphere from the chelated precursor, spray pyrolysed at 850 °C.

3.2.2. Phase identification and chemical purity

Powders of both precursors from spray pyrolysis were X-rayed at different pyrolysis temperatures for their

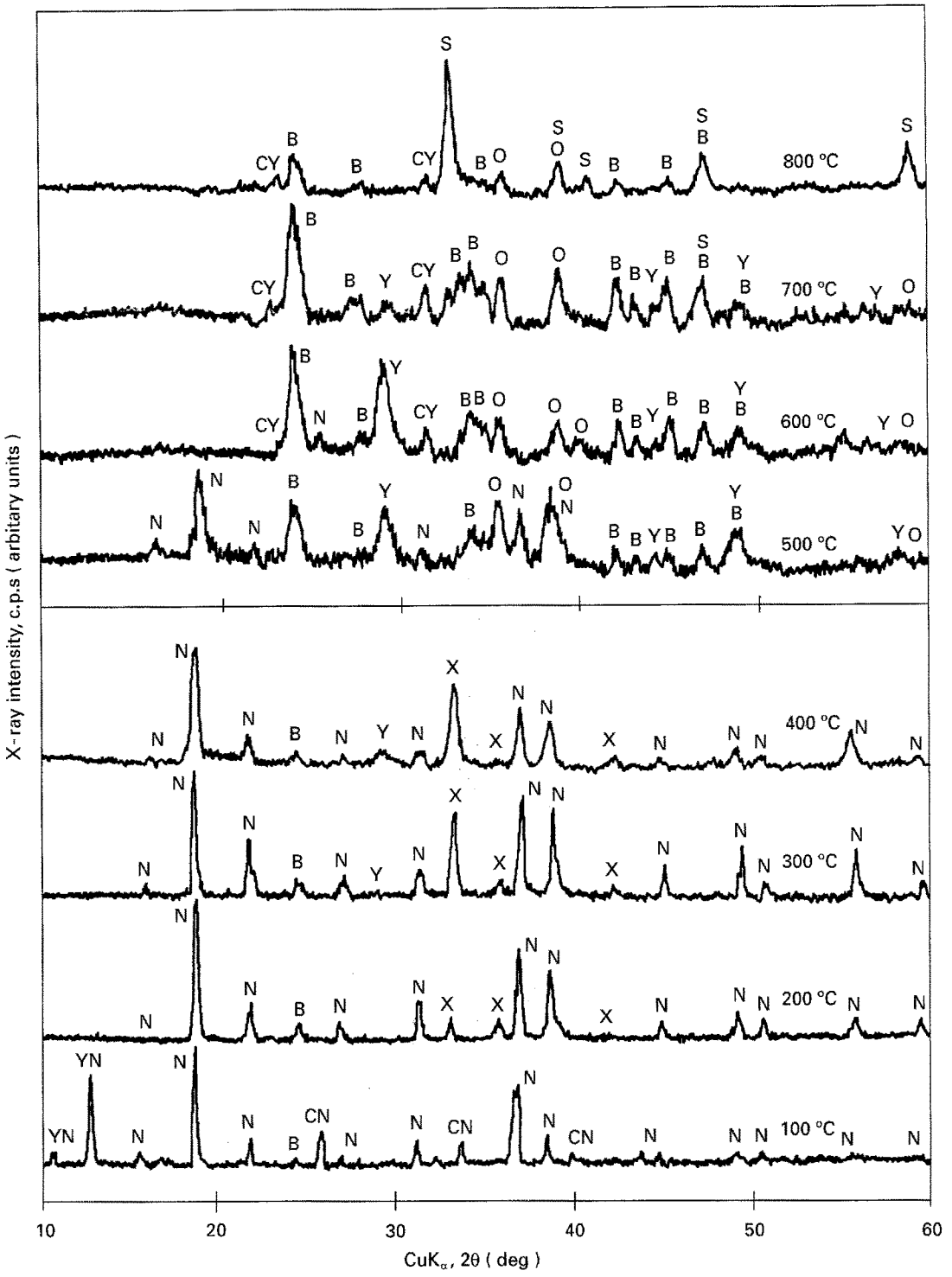

Figure 7 X-ray diffraction patterns of thermally decomposed nitrate precursors at 100–800 °C: (CY) $Cu_2Y_2O_5$, (S) $YBa_2Cu_3O_7$, (O) CuO, (N) $Ba(NO_3)_2$, (B) $BaCO_3$, (Y) Y_2O_3, (CN) Cu $(NO_3)_{3x}$ H_2O, (YN) $Y(NO_3)_3$ $6H_2O$, (X) Cu $(OH)_x$ $(NO_3)_y$.

phase identification. The XRD patterns also served as indicators of the reactivity of the precursors. Powders of the superconducting phase formed, from chelated precursors at 800–1000 °C, by ultrasonic spray pyrolysis (Fig. 13). For nitrate precursors, powders of superconducting phase formed from 900 to 1000 °C (Fig. 14). The FTIR spectra of these powders showed the infrared transparency characteristic of the Y–Ba–Cu–O superconducting phase [31].

Qualitative energy dispersive spectra of the spray pyrolysed powders from both precursors determined the chemical purity of these powders.

3.2.3. Particle formation mechanism

The particle formation mechanism can be described as follows. The mist droplets of the solution that were atomized by an ultrasonic transducer were passed through a furnace where first, plastic crusts developed on the droplets as they were being dried. Further heating caused the vapour pressure inside the crust to increase, expanding the droplets. Vapours that escaped the crusts formed very tiny particles, called primary particles. The droplets that were unchanged until decomposition, were called secondary particles. Some droplets were blown up and/or ignited according to the chelating agent used. The droplet fragments

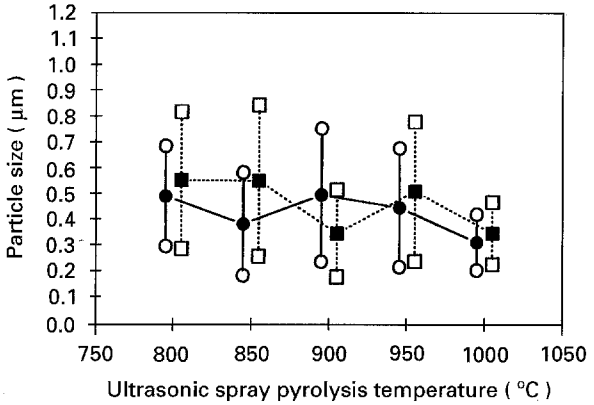

Figure 8 The variation of the median size and size range of the spray pyrolysed particles from (■) nitrate and (●) chelated precursors versus temperature.

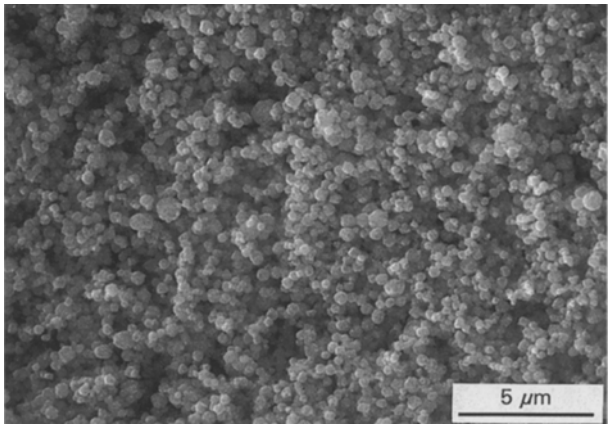

Figure 9 SEM photomicrograph of powders from the chelated precursors by ultrasonic spray pyrolysis at 1000 °C show the uniform particle size distribution of the powders.

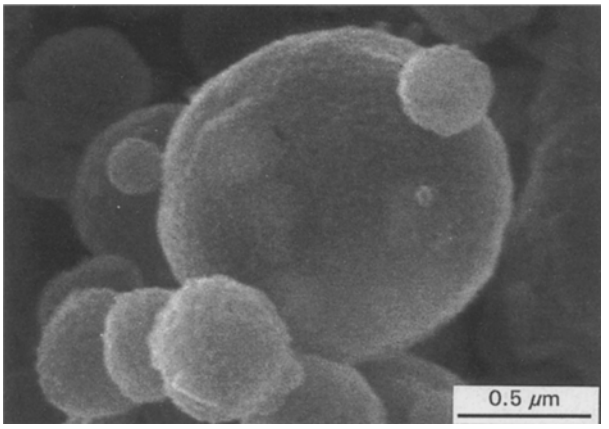

Figure 10 SEM photomicrograph of powder from a chelated precursor by ultrasonic spray pyrolysis at 800 °C shows the primary, secondary and final particles.

were then spherodized if the temperature was high enough. Secondary particles formed from the vapour or the fragments. Agglomerates formed from secondary particles either spherical or irregular in shape depending upon the temperature.

4. Conclusions

For the chelated solution with a pH 8, FTIR suggested bidentate bonding between the cations and the citric

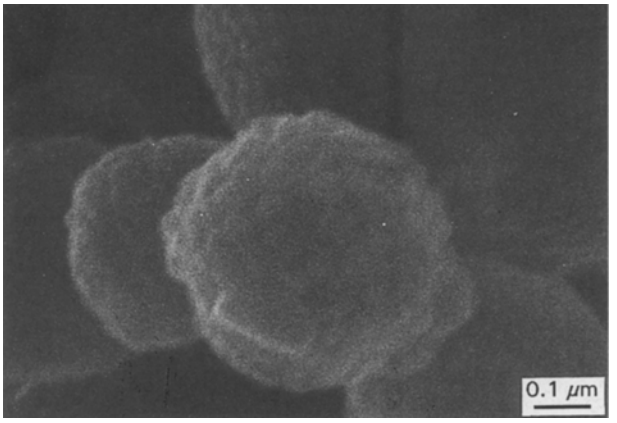

Figure 11 SEM photomicrograph of powder from a chelated precursor by ultrasonic spray pyrolysis at 800 °C shows secondary particles that consist of small crystallites of primary particle size.

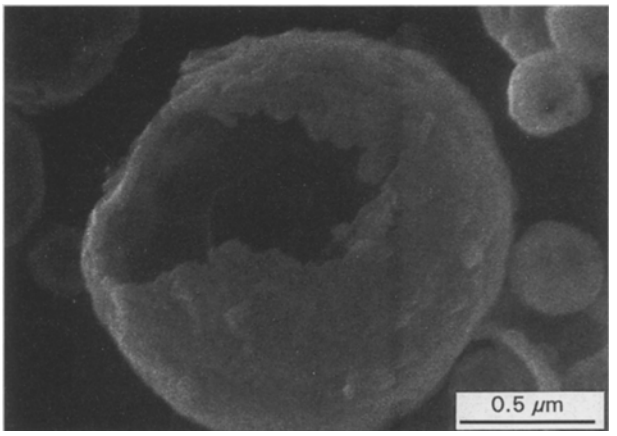

Figure 12 SEM photomicrograph of powder from a chelated precursor by ultrasonic spray pyrolysis at 850 °C showing a blown-out hollow sphere.

radicals. XRD showed that the dried gel was nearly amorphous with a weak barium nitrate peak. Both results suggest intimate mixing at the atomic level. FTIR and XRD studies versus temperatures revealed the decomposition and forming mechanisms of the precursor and superconducting phase, respectively.

Ultrasonic spray pyrolysis formed powders of the superconducting phase at 800–1000 °C from chelated precursors. This is about 100 °C lower than those from the nitrate solutions due to the chelation effect. SEM studies showed that spray pyrolysed powders are hollow multicrystalline spheres after spray pyrolysis at temperatures below 950 °C, and are solid particles at temperatures above 950 °C due to the melting of the hollow particles. Microscopic studies also showed that the particles have sizes from 0.2 to 0.5 μm, with crystallite size at about 0.01–0.05 μm. EDX indicated no significant chemical contamination.

Ultrasonic spray pyrolysis of the chelated precursors has been shown to have the advantages of a lower reaction temperature, spherical particles, with control of the particle size and particle size distribution with potential for wide application to many multicomponent systems, with the further advantage of being easy to scale up for industrial use.

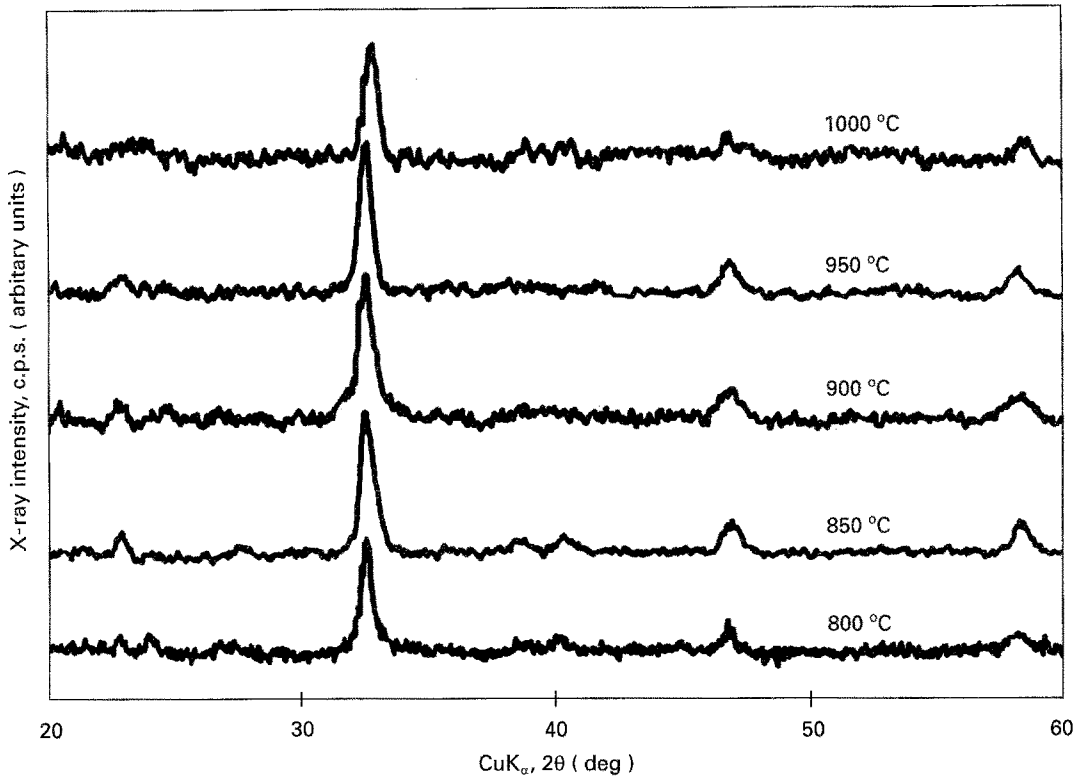

Figure 13 X-ray diffraction patterns of powders from chelated precursors spray pyrolysed at 800–1000 °C.

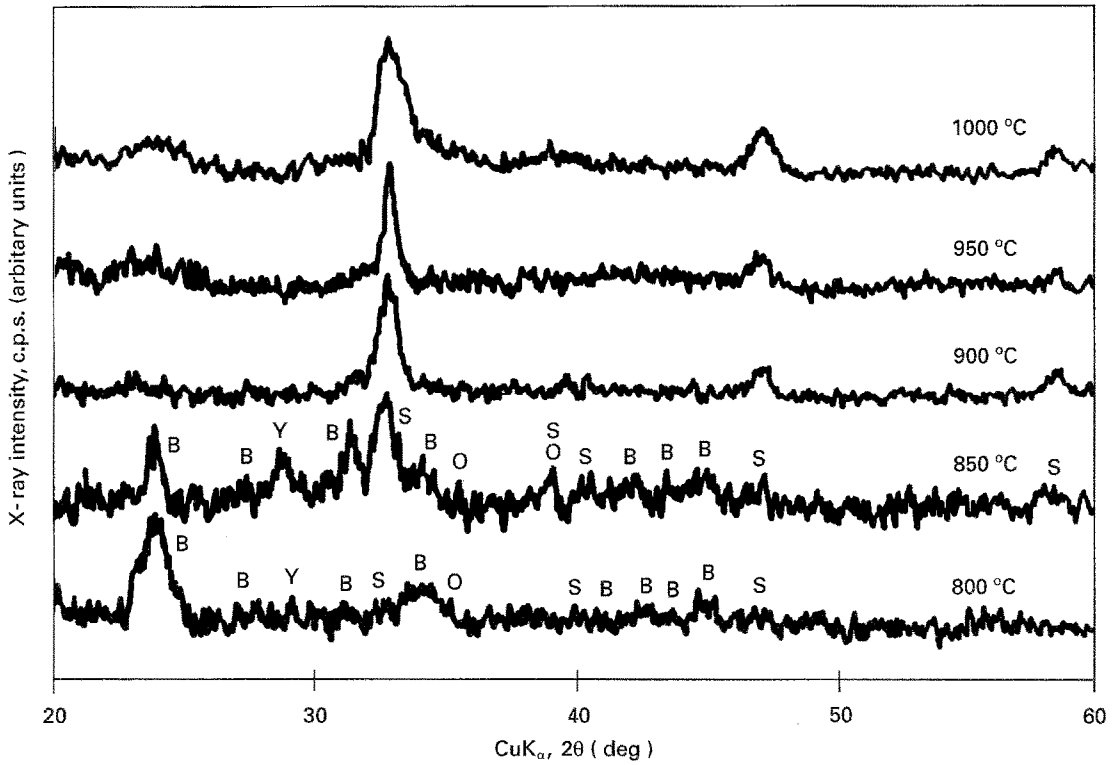

Figure 14 X-ray diffraction patterns of powders from nitrate precursors spray pyrolysed at 800–1000 °C. (Y) Y_2O_3, (S) $YBa_2Cu_3O_7$, (O) CuO, (B) $BaCO_3$.

References

1. M. F. YAN, *Mater. Sci. Eng.* **48** (1981) 53.
2. W. D. KINGERY, in "Ceramic Powders", edited by P. Vincenzini, Material Science Monographs, Vol. **16** (Elsevier, Amsterdam, 1983) p. 3.
3. B. C. BUNKER, J. A. VOIGT, D. L. LAMPPA, D. H. DOUGHTY, E. L. VENTURINI, J. F. KWAK, D. S. GINLEY, T. J. HEADLEY, M. S. HARRINGTON, M. O. EATHOUGH, R. G. TISSOT JR., and W. F. HAMMETTER, *Mater. Res. Soc. Symp. Proc.* **121** (1988) 373.
4. M. MURATA and K. WAKINO, *Mater. Res. Bull.* **11** (1976) 323.
5. R. W. SCHWARTZ, D. J. EICHORST and D. A. PAYNE, *Mater. Res. Soc. Symp. Proc.* **73** (1986) 123.
6. R. LEGROS, R. METZ, J. P. CAFFIN, A. LAGRANGE and A. ROUSSET, *ibid.* **121** (1988) 251.

7. L. V. INTERRANTE, *et al.*, in "Chemistry of High-Temperature Superconductors", edited by D. L. Nelson and T. F. George, American Chemical Society, Washington DC (1988) p. 169.
8. C. C. CHENG, Ms Thesis, University of Missouri-Rolla (1988).
9. M. INOUE, E. TAKASE, Y. TAKAJ and H. HAYAKAWA, *Jap. J. Appl. Phys.* **28** (1989) L1575.
10. T. FUJISAWA, A. TAKAGI, T. HONJOH, K. OKUYAMA, S. OSHIMA and K. MATSUKI, *ibid.* **28** (1989) 1358.
11. H. MEERWEIN and T. BERSIN, *Ann.*, **476** (1929) 113.
12. P. P. PHULE and S. H. RISBUD, *Mater. Res. Soc. Symp. Proc.* **121** (1988) 275.
13. M. A. ACCIBAL, J. W. DRAXTON, A. H. GABOR, W. L. GLADFELTER, B. A. HASSLER and M. L. MECARTNEY, *ibid.* **401** (1988).
14. J. C. BERNIER, J. L. REHSPRINGER, S. VILMINOT and P. POIX, *ibid.* **73** (1986) 129.
15. E. MATIJEVIC, *Acc. Chem. Res.* **14** (1981) 22.
16. H. IMAI, K. TAKAMI and M. NAITO, *Mater. Res. Bull.* **19** (1984) 1293.
17. T. J. GARDNER and G. L. MESSING, *Ceram. Bull.* **63** (1984) 1498.
18. T. J. GARDNER, D. W. SPROSON and G. L. MESSING, *Mater. Res. Soc. Symp. Proc.* **32** (1984) 227.
19. D. W. SPROSON, G. L. MESSING and T. J. GARDNER, *Ceram. Int.* **12** (1986) 3.
20. K. S. MAZDIYASNI, C. T. LYNCH and J. S. SMITH, *J. Amer. Ceram. Soc.* **48** (1965) 372.
21. H. ISHIZAWA, O. SAKURAI, N. MIZUTANI and M. KATO, *Amer. Ceram. Soc. Bull.* **65** (1986) 1399.
22. Y. KANNO and T. SUZUKI, *J. Mater. Sci.* **23** (1988) 3067.
23. D. W. JOHNSON Jr, *Amer. Ceram. Soc. Bull.* **60** (1981) 221.
24. B. DUBOIS, D. RUFFIER and P. ODIER, *J. Amer. Ceram. Soc.* **72** (1989) 713.
25. T. T. KODAS, E. M. ENGLER, V. Y. LEE, R. JACOWITZ, T. H. BAUM, K. ROCHE, S. P. PARKIN, W. S. YOUNG, J. KLEDER and W. AUSER, *Appl. Phys. Lett.* **52** (1988) 1622.
26. N. TOHGE, M. TATSUMISAGO, T. MINAMI, K. OKUYAMA, M. ADACHI and Y. KOUSAKA, *Jap. J. Appl. Phys.* **27** (1988) L1086-8.
27. G. SCHNITTGRUND, "Reproducible Large-Scale Production of Thallium-Based High-Temperature Superconductors", Rockwell International Corp., Rocketdyne Division (1989).
28. L. M. SHEPPARD, *Ceram. Bull.* **70** (1991) 1484.
29. S. C. ZHANG, and G. L. MESSING, in "Ceramic Powder Science III", edited by G. L. Messing, S. Hirano and H. Hausner (The American Ceramic Society, Westerville, OH, 1990).
30. R. L. PESKIN and R. J. RACO, *J. Acoust. Soc. Amer.* **35** (1963) 1378.
31. C. LIAO, X. CHEN, D. DU and X. QI, *Mod. Dev. Powder Metall.* **18** (1988) 789.

Received 10 March
and accepted 24 May 1995